

Polaronic and nonadiabatic phase diagram from anomalous isotope effects

P. Paci¹, M. Capone², E. Cappelluti², S. Ciuchi³, C. Grimaldi⁴ and L. Pietronero¹

¹Dipartimento di Fisica, Università di Roma "La Sapienza", and INFN UdR RM1, 00185 Roma, Italy

²"Enrico Fermi" Research Center, c/o Compendio del Viminale, and INFN UdR RM1, 00184 Roma, Italy

³Dipartimento di Fisica, Università de L'Aquila, and INFN UdR AQ, 67010 Coppito-L'Aquila, Italy and

⁴Laboratoire de Production Microtechnique, Ecole Polytechnique Fédérale de Lausanne, CH-1015 Lausanne, Switzerland

(dated: March 22, 2024)

Isotope effects (IEs) are a powerful tool to probe directly the dependence of many physical properties on the lattice dynamics. In this paper we investigate the onset of anomalous IEs in the spinless Holstein model by employing the dynamical mean field theory. We show that the isotope coefficients of the electron effective mass and of the dressed phonon frequency are sizeable also far away from the strong coupling polaronic crossover and mark the importance of nonadiabatic lattice fluctuations in the weak to moderate coupling region. We characterize the polaronic regime by the appearance of huge IEs. We draw a nonadiabatic phase diagram in which we identify a novel crossover, not related to polaronic features, where the IEs attain their largest anomalies.

PACS numbers: 71.38.-k, 63.20.Kr, 71.38.Cn, 71.38.Ht

The relevant role of electron-phonon (el-ph) interactions on the properties of complex materials as the high- T_c superconductors has been recently revived by a number of experiments. In particular, the finite, and yet unexplained, anomalous IEs on the penetration depth [1], on the pseudogap temperature [2], and on the angle-resolved photoemission spectra [3] in high- T_c superconductors open a new challenge in the understanding the role of the el-ph interaction in these materials. Sizable isotope effects on magnetic and charge-ordering critical temperatures in manganites point out the relevance of the el-ph coupling also in these materials [4].

Despite that the el-ph problem has been thoroughly studied and that many of its manifestations are now well understood, only few partial studies have been devoted to IEs and to their significance in relation to the underlying nature of the el-ph interaction [5, 6]. Yet, the prediction and observation of IEs on different physical properties represent a powerful tool to assess the role of the el-ph interaction in many materials. For instance, the finite isotope shift on the penetration depth [1], and hence indirectly on the effective electron mass m^* , is of particular interest since it contrasts the conventional Migdal-Eliashberg (ME) scenario which predicts strictly zero IE on this quantity. In this perspective the understanding of finite IEs on m^* cannot rely on the ME framework and more general approaches are then required.

A modern tool of investigation which overcomes the limitations of ME theory is the so-called dynamical mean field theory (DMFT), a nonperturbative method which neglects spatial correlations in order to fully account for local quantum dynamics, and becomes exact in the infinite coordination limit [7]. In the case of el-ph interactions, this approach allows us to study with equal accuracy all coupling regimes, and to fully include phonon quantum fluctuations which are only partially taken into account in ME approach according to Migdal's theorem. DMFT has been successfully em-

ployed in the study of multiphonon effects, polaron instabilities, metal-insulator transitions (MIT) as well as quasiparticle regimes in the Holstein electron-phonon system [8, 9, 10, 11].

Considering the Holstein model as a paradigmatic lattice model for el-ph interaction, we discuss the anomalies of the IEs on electronic and phononic properties arising in purely el-ph systems. We employ DMFT to span the whole phase diagram determined by the dimensionless el-ph coupling λ and by $\beta = \hbar\omega_0/t$, the "adiabatic" ratio between the phonon energy $\hbar\omega_0$ and the electron hopping rate t . Increasing β gradually induces a crossover from free carriers to polarons with reduced mobility, while λ measures the relevance of quantum lattice fluctuations. Particular attention will be paid on the dependence of the IEs on the quantum lattice fluctuations triggered by the finite adiabatic parameter $\beta \neq 0$.

We show that a sizable negative isotope coefficient on the electronic mass m^* characterizes the whole parameter range, while a divergence of m^* is recovered only approaching the MIT polaron transition at λ_c and $\beta = 0$. Similar features are found for the renormalized phonon frequency ω_0 which displays an isotope coefficient α_0 significantly different from the ME limit $\alpha_0 = 1/2$. Based on the dependence of the isotope coefficients on the adiabatic ratio β , we draw a phase diagram wherein we identify, beside the strong-coupling polaronic regime [10]: i) a nonadiabatic perturbative regime where IEs increase with β , and ii) a complex nonadiabatic regime where the anomalies of the IEs decrease with β and approach the Lang-Firsov predictions in the $\beta \rightarrow \infty$ limit.

In this paper we are interested in the continuous evolution of the el-ph properties from the quasiparticle to the polaronic regime. It is well known that the Holstein model undergoes various instabilities leading to superconductivity, charge-density-wave ordering and bipolaron formation [12]. In order to focus on the metallic properties and to clarify the origin of anomalous IEs in this

regime, we consider here a half-filled spinless Holstein model, which enforces the metallic character in the whole k -space (for $\epsilon = 0$) [10]. Our Hamiltonian reads:

$$H = \sum_{i,j} t_{ij} c_i^\dagger c_j + g \sum_i n_i (a_i + a_i^\dagger) + \frac{1}{2} \sum_i \omega_0 a_i^\dagger a_i; \quad (1)$$

where c_i^\dagger (c_i), a_i^\dagger (a_i) are creation (annihilation) operators for electrons and phonons on site i , respectively, $n_i = c_i^\dagger c_i$ is the electron density and g is the electron-phonon matrix element.

The physical properties of (1) are governed by two microscopic parameters: the electron-phonon coupling $\lambda = 2g^2/\omega_0 t$ and the adiabatic ratio $\gamma = \omega_0/t$. The standard Landau Fermi-liquid (FL) picture is sustained by the ME theory in the adiabatic limit $\gamma = 0$ for $\lambda < \lambda_c$, while for $\lambda > \lambda_c$ the FL regime is destroyed due to the polaron localization. For $\gamma > 0$, this sharp transition becomes a smooth crossover between well and poorly defined quasiparticle properties. This rich phenomenology is reflected in the appearances of anomalous EEs on various quantities. Let us consider for example the isotope coefficient on the effective electron mass $m^* = d \ln(m^*)/d \ln(M)$, where M_p is the ionic mass. Since $g/\omega_0 = M/\omega_0$ and $\omega_0/\omega_0 = M$, the electron-phonon coupling is independent of M and m^* can be rewritten as:

$$m^* = \frac{1}{2} \frac{d \ln(m^*)}{d \ln(\lambda)}; \quad (2)$$

According to the FL description, m^* can be expressed in terms of a mass-enhancement factor f_m :

$$m^* = 1 + f_m(\lambda, \gamma); \quad (3)$$

In the adiabatic regime $\gamma = 0$, f_m can be expanded in powers of λ , $m^* = 1 + f_m(\lambda; 0) + f_m^1(\lambda)$, and hence

$$m^* = \frac{m}{2m} f_m^1(\lambda); \quad (4)$$

The isotope coefficient thus increases with λ and it correctly reproduces the ME result $m^* = 0$ when $\lambda = 0$. Such an increase is indeed found by calculations based on a perturbative expansion in λ [5, 6], whose validity is however limited only to weak λ values. In the opposite antiadiabatic limit $\gamma \rightarrow 1$ the Holstein-Lang-Firsov approximation gives $m^* = \exp(\lambda/2)$, leading to

$$m^* = \frac{\lambda}{4}; \quad (5)$$

which decreases as λ gets higher, as opposed to the previous case of Eq. (4). The two limiting cases for $\gamma = 0$ and $\gamma = 1$ suggest that for fixed $\lambda < \lambda_c$ the strongest isotope shifts lie in the intermediate nonadiabatic region $\gamma < 1$, which can be investigated only by non-perturbative tools as the DMFT approach.

In this work we consider (1) on an infinite coordination Bethe lattice and use exact diagonalization (ED) to

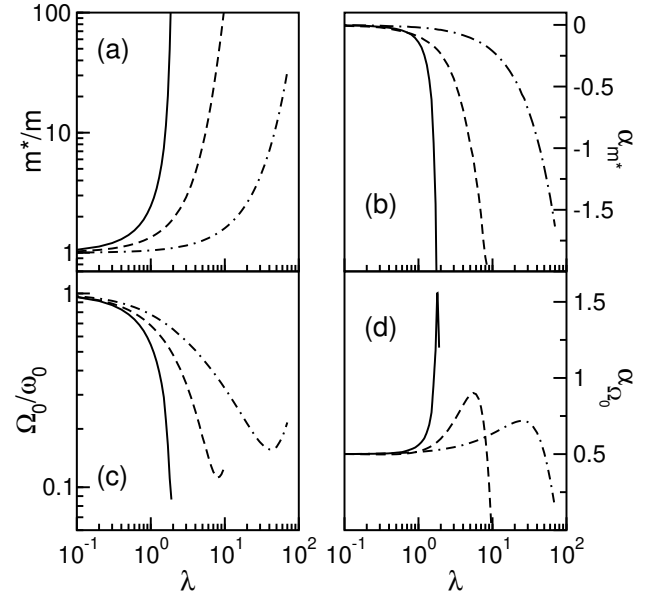


FIG. 1: Effective electron mass $m^* = m$ (a) and renormalized phonon frequency $\omega_0 = \omega_0$ (c) as function of λ for $\gamma = 0.1$ (solid line), $\gamma = 1$ (dashed line) and $\gamma = 10$ (dot-dashed line). The corresponding isotope coefficients are shown in panels b,d.

solve the impurity problem that DMFT associates to the lattice model [7, 13]. As customary, the Anderson model is truncated by considering N_s impurity levels, and a cutoff on the phonon number is imposed on the infinite phonon Hilbert space. The DMFT self-consistency is implemented in the Matsubara frequencies $\omega_n = (2n+1)\pi T$ where T is a fictitious temperature. The evaluation of EEs is a particularly difficult task since it requires a high accuracy on both the electron and phonon properties and of their dependence on λ . In particular, a number of phonon states up to 100 and T as small as $1/1600$ were needed to ensure reliable and robust results. The number of impurity levels has been fixed at $N_s = 9$, having checked that no significant change occurred for larger N_s . We compute the electron self-energy $\Sigma(\omega_n)$ and the phonon Green's function $D(\omega_n)$ which yield the effective electron mass $m^* = 1 - \text{Re}(\Sigma(\omega_n=0))/t$ and the renormalized phonon frequency ω_0 as $(\omega_0/\omega_0)^2 = -2\text{Re}(\omega_n=0)/\omega_0$. The corresponding isotope coefficients are obtained by means of a finite shift $\lambda = 0.15$.

In Fig. 1 we show m^* and ω_0/ω_0 and their corresponding isotope coefficients as a function of the electron-phonon coupling λ for $\gamma = 0.1; 1; 10$ which are representative respectively of the quasi-adiabatic, nonadiabatic and antiadiabatic regimes. The polaron crossover is reflected in a strong enhancement of m^* as λ increases. The crossover occurs at $\lambda = 1.18$ for $\gamma = 0$, and moves to larger coupling as γ increases, until the antiadiabatic regime, in which the crossover roughly occurs when the average number of phonons $\bar{n} = \lambda/2 > 1$ [8, 10, 14]. As a consequence, at fixed λ the effective mass becomes

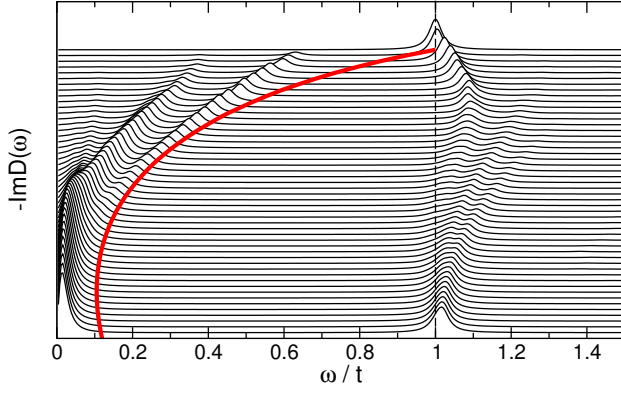


FIG. 2: (color online) Phonon spectral function (solid lines) for different values of the el-ph coupling γ from 0 to 10 with steps of 0.2. The thick red line represent the renormalized phonon frequency ω_0 and the thin dashed line ω'_0 .

smaller as γ increases, implying a negative isotope coefficient α_m as reported in Fig.1 (b). The polaron regime is thus identified by the huge negative values of α_m . Just as in the case of $m = m_0$, increasing γ makes the variation of α_m smoother and shifts it to larger γ .

A similar behavior is found for the renormalized phonon frequency ω_0 , as shown in Fig.1 (c), where the polaron instability is reflected in a sharp phonon softening in the quasi-adiabatic case ($\gamma = 0.1$) close to polaron crossover. Once again, the softening is weaker as γ gets larger. For fixed γ this leads to an anomalous isotope coefficient $\alpha_0 > 1/2$, as reported in Fig.1 (d).

Some words are worth to be spent about the apparent phonon hardening accompanied by the corresponding decreasing of ω_0 as reported in Figs.1 (c,d) for large γ . This anomalous phonon feature is just a consequence of our "static" definition of renormalized phonon frequency ($\omega_0 = \omega'_0$)² = $2D^{-1}(\omega'_m = \omega'_0) = \omega'_0$. This definition corresponds to describe the full phonon spectrum as a single δ -function at frequency $\omega'_0 = 1/(\omega'_0)$ and $\text{Im}D(\omega'_0 + i0^+) = 0$. Such description becomes less representative as the spectral function acquires a complex structure.

In Fig.2 we report the evolution of the phonon spectral function by increasing the el-ph coupling for $\gamma = 1$. The real frequency phonon propagator is directly computed in the ED scheme. Note that only gross features can be extracted because of the discreteness of the impurity model. The average phonon softening (thick red line) at small γ stems from a transfer of spectral weight from ω'_0 to a low energy peak which exponentially approaches $\omega'_0 = 0$. An opposite behavior occurs for strong el-ph coupling where the lattice potential is a double-well with energy barrier $E_b \gg \omega'_0$. This gives rise to a second peak at frequency ω'_0 yielding a hardening of the averaged phonon frequency ω_0 . Similar considerations lead to the decrease at large γ of the IE α_0 .

The study of the dependence of $m = m_0$, ω_0 and their

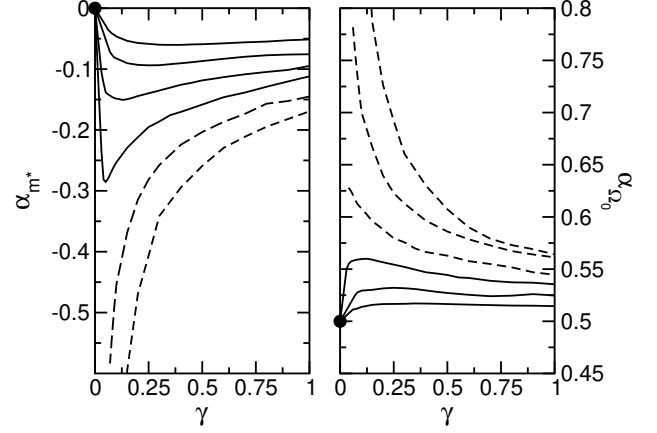


FIG. 3: Dependence of α_m and α_0 on the nonadiabatic parameter γ . Curves are plotted for the el-ph coupling $\gamma = 0.6; 0.8; 1.0; 1.2; 1.4; 1.6$ from top to bottom (bottom to top) in left (right) panel. Filled black circles mark the adiabatic M E limit.

respective IEs highlights in the clearest way the appearance of giant IEs close to the polaronic crossover. However, interesting anomalies and sizeable deviations of IEs from M E predictions appear far from polaronic regime in a region where the system preserves good metallic properties. These anomalous features can thus be connected to the onset of nonadiabatic effects in the el-ph properties in the spirit of a generalization of the FL liquid picture as in Eq.(3) [5, 15, 16]. To this aim we analyze in more details the dependence of the IEs on the quantum lattice fluctuations triggered by the finite adiabatic parameter $\gamma \neq 0$. In Fig. 3 we plot the γ -dependence of α_m and α_0 for different el-ph coupling ranging from weak ($\gamma = 0.6$) to intermediate-strong coupling ($\gamma = 1.6$). Two qualitatively different behaviors marked by the solid and dashed lines are identified. Dashed lines represent strong coupling values for which the system undergoes a polaronic MIT for $\gamma \neq 0$ signaled by the divergence of the isotope coefficients. Solid lines are representative of weak-to-moderate values for which the system maintains its FL metallic character with isotope coefficients recovering their standard M E values $\alpha_m = 0$ and $\alpha_0 = 1/2$ as $\gamma \rightarrow 0$. Note that for $\gamma = 1.2$ we find that $\alpha_m \neq 0$ and $\alpha_0 \neq 1/2$ for $\gamma \neq 0$, in agreement with Ref. [11] which predicts two different critical values $\gamma_c^{ph} = 1.18$ and $\gamma_c^{el} = 1.328$ where a double-well lattice potential and an electronic self-trapping respectively occur.

The different physics underlying the regimes sketched by dashed and solid lines is reflected in the overall dependence of the IEs. In the large coupling regime $\gamma > \gamma_c$ the isotope coefficients diverge for $\gamma \neq 0$ and approach monotonically zero in the antiadiabatic limit. For $\gamma < \gamma_c$ on the other hand we find a more complex behavior with an initial increase of the anomalies of α_m and α_0 as function of γ up to a certain value γ^* , above which the

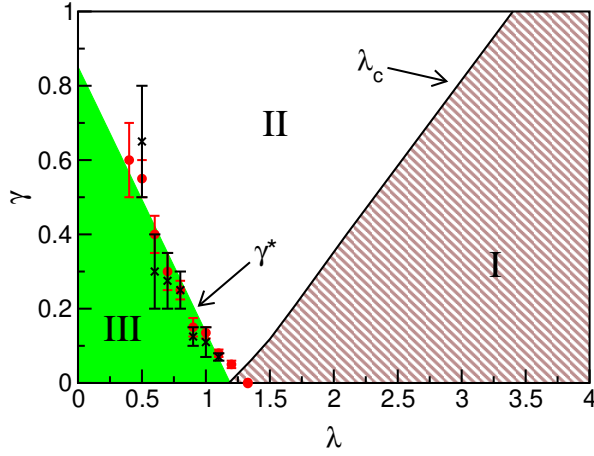


FIG. 4: (color online) Nonadiabatic phase diagram defined by anomalous IEs. Filled red circles and black crosses represent respectively the minimum and the maximum in the behavior of γ_m, γ_0 . Error bars are not related to the accuracy of the isotope coefficients but more to the flatness of γ_m, γ_0 as function of λ . The curve γ_c marks the polaron crossover as defined in the text.

anomalies decrease and disappear in the antiadiabatic limit in agreement with the Lang-Firsov predictions. In the nonadiabatic crossover region ($\lambda < \lambda_c$ and $\gamma > \gamma_c$) significant anomalies of the IEs $\gamma_m \approx 0.3$ and $\gamma_0 \approx 0.55$ are observed even in the metallic regime far from the polaronic instability. It is worth to stress that the values of γ strongly depends on the el-ph coupling and that in principle a nonadiabatic crossover parameter can be defined for both the electronic and phononic properties.

As discussed above, the curve γ_c separates a region in which a perturbative theory based on the adiabatic FL picture can be safely employed ($\lambda < \lambda_c$) from a region where the Lang-Firsov approach is a more appropriate starting point for a $1/\lambda$ expansion ($\lambda > \lambda_c$). However around λ_c at $\gamma = 0$ both ME and Lang-Firsov approaches are expected to fail due to strong entanglement of electron and phonon degrees of freedom [8].

The complex phenomenology of the IEs in the whole λ - γ phase diagram is summarized in Fig. 4, where the nonadiabatic crossover is defined respectively by the minimum (filled circles) and maximum (crosses) of the γ_m, γ_0 as functions of λ . We note that, apart from a very small region close to the adiabatic limit, γ lies on an universal curve for both the electron and phonon properties reflecting the fact that electron and lattice degrees of freedom are strictly mixed in the nonadiabatic regime. This is indeed not true for $\gamma = 0$ where γ disappear at the two different values $\gamma_c^{ph}, \gamma_c^{el}$ above discussed. It is also worth to stress that the nonadiabatic crossover, pointed out by the dependence of the anomalous isotope effects, is not related to the onset of polaronic effects, as shown in Fig. 4 where the polaron crossover at finite γ is here

pinpointed by the appearance of a bimodal structure in the lattice probability distribution function. For $\lambda > \lambda_c$ the polaron crossover is reflected in a strong degradation of the metallic properties with an almost vanishing coherent spectral weight. The behaviors of γ_c and γ_c^* define three regimes which can be roughly described as: I) a polaron region (brown dashed area in Fig. 4) where electrons are almost trapped leading to significant lattice distortions. This effect is strongly removed by the lattice quantum fluctuation triggered by a finite γ leading to giant IEs; II) a highly nonadiabatic region (white area) where the system is qualitatively described in terms of itinerant quasi-particle carrying along its hugely fluctuating phonon cloud. In this regime quantum lattice fluctuations relax the mixing between lattice and electronic degrees of freedom leading to a reduction of the anomalous IEs; III) a weakly nonadiabatic region (grey filled area) where anomalous IEs are tuned by the opening of nonadiabatic channels in the el-ph interaction. In this region DMFT qualitatively confirms the results of the nonadiabatic theory described by vertex diagrams in a perturbative approach [5, 15].

In conclusion we have defined a phase diagram of the spinless Holstein model based on the anomalous phenomenology of the IEs on both electronic and phonon properties. In the metallic regime we identified a new nonadiabatic crossover (not related to polaronic instability) between different weakly and highly nonadiabatic FL quasiparticle picture. The largest anomalies in the isotope coefficients are found in this intermediate crossover region. Experimental investigations of anomalous IEs on different physical properties represent thus a powerful tool to probe the complex nature of the el-ph interaction in real materials. Theoretical studies based on Density Functional Theory predict $A_{3C_{60}}$ fullerides, cuprates and MgB_2 to be roughly in the nonadiabatic crossover where the anomalies in the IEs are the most sizable. A rigorous generalization of our results in the presence of electronic correlation and away from the half-filling case is of course needed for quantitative analysis in these complex materials. Preliminary results show that γ_m can be significantly suppressed in low filled systems even in highly nonadiabatic regime, in agreement with recent experimental results in MgB_2 [17].

We are grateful to C. Castellani for illuminating discussions. We acknowledge financial support from Miur Co n2003 and FIRB RBAU017S8R and INFN PRA-UMBRA.

-
- [1] G. M. Zhao et al., Nature (London) 385, 236 (1997); R. Khasanov et al., Phys. Rev. Lett. 92, 057602 (2004).
 - [2] D. Rubio Temprano, et al., Phys. Rev. Lett. 84, 1990 (2000).
 - [3] G. H. Gweon, T. Sasagawa, S. Y. Zhou, H. Takagi, D. H.

- Lee, A. Lanzara, unpublished.
- [4] G. Zhao, K. Conder, H. Keller, and K. A. Müller, *Nature* 381, 676 (1996).
- [5] C. Grimaldi, E. Cappelluti, and L. Pietronero, *Europhys. Lett.* 42, 667 (1998).
- [6] A. Deppeler and A. J. M. Illis, *Phys. Rev. B* 65, 224301 (2002).
- [7] A. Georges, G. Kotliar, W. Krauth, and M. J. Rozenberg, *Rev. Mod. Phys.* 68 13 (1996).
- [8] S. Ciuchi, F. de Pasquale, S. Fratini, and D. Feinberg *Phys. Rev. B* 56, 4494 (1997).
- [9] D. Meyer, A. C. Hewson, and R. Bulla, *Phys. Rev. Lett.* 89, 196401 (2002).
- [10] M. Capone and S. Ciuchi, *Phys. Rev. Lett.* 91, 186405 (2003).
- [11] A. J. M. Illis, R. Müller, and B. I. Shraiman, *Phys. Rev. B* 54, 5389 (1996).
- [12] J. K. Freericks et al., *Phys. Rev. B* 48, 6302 (1993).
- [13] M. Caruel and W. Krauth, *Phys. Rev. Lett.* 72, 1545 (1994).
- [14] M. Capone, W. Stephan, and M. Grilli, *Phys. Rev. B* 56, 4484 (1997); M. Capone, C. Grimaldi, and S. Ciuchi, *Europhys. Lett.* 42, 523 (1998).
- [15] C. Grimaldi, L. Pietronero, and S. Strassler, *Phys. Rev. Lett.* 75, 1158 (1995).
- [16] E. Cappelluti, C. Grimaldi, L. Pietronero, and S. Strassler, *Phys. Rev. Lett.* 85, 4771 (2000).
- [17] D. DiCastro et al., cond-mat/0307330 (2003).